Vibrational Spectroscopy Reveals Electrostatic and Electrochemical Doping in Organic Thin Film Transistors Gated with a Polymer Electrolyte Dielectric

ARTICLE *in* JOURNAL OF THE AMERICAN CHEMICAL SOCIETY · JULY 2007

Impact Factor: 12.11 · DOI: 10.1021/ja070615x · Source: PubMed

5 AUTHORS, INCLUDING:

Loren Kaake
University of California, Santa Barbara
18 PUBLICATIONS **803** CITATIONS
SEE PROFILE

Ying Zou
Shanghai Institute of Applied Physics
49 PUBLICATIONS **867** CITATIONS
SEE PROFILE

C. Daniel Frisbie
University of Minnesota Twin Cities
225 PUBLICATIONS **14,583** CITATIONS
SEE PROFILE

J|A|C|S
ARTICLES
Published on Web 06/01/2007

Vibrational Spectroscopy Reveals Electrostatic and Electrochemical Doping in Organic Thin Film Transistors Gated with a Polymer Electrolyte Dielectric

L. G. Kaake, Y. Zou, M. J. Panzer, C. D. Frisbie, and X.-Y. Zhu*

Contribution from the Departments of Chemistry and Chemical Engineering and Materials Science, University of Minnesota, Minneapolis, Minnesota 55455

Received January 27, 2007; E-mail: zhu@chem.umn.edu

Abstract: We apply attenuated total internal reflection Fourier transform infrared (ATR-FTIR) spectroscopy to directly probe active layers in organic thin film transistors (OTFTs). The OTFT studied uses the *n*-type organic semiconductor *N*-*N*′-dioctyl-3,4,9,10-perylene tetracarboxylic diimide (PTCDI-C8) and a polymer electrolyte gate dielectric made from poly(ethylene oxide) and $LiClO_4$. FTIR spectroscopy of the device shows signatures of anionic PTCDI-C8 species and broad polaron bands when the organic semiconductor layer is doped under positive gate bias (V_G). There are two distinctive doping regions: a reversible and electrostatic doping region for $V_G \leq 2$ V and an irreversible and electrochemical doping regime for $V_G > 2$ V. On the basis of intensity loss of vibrational peaks attributed to neutral PTCDI-C8, we obtain a charge carrier density of $2.9 \times 10^{14}/cm^2$ at $V_G = 2$ V; this charge injection density corresponds to the conversion of slightly more than one monolayer of PTCDI-C8 molecules into anions. At higher gate bias voltage, electrochemical doping involving the intercalation of Li^+ into the organic semiconductor film can convert all PTCDI-C8 molecules in a 30-nm film into anionic species. For comparison, when a conventional gate dielectric (polystyrene) is used, the maximum charge carrier density achievable at $V_G = 200$ V is $\sim 4.5 \times 10^{13}/cm^2$, which corresponds to the conversion of 18% of a monolayer of PTCDI-C8 molecules into anions.

Introduction

Charge transport at or across interfaces is central to the operation of a wide variety of molecule-based devices, including organic light-emitting diodes, organic thin film transistors (OTFT), organic photovoltaic cells, and nanoscopic molecular junctions based on single molecules or a small assembly of molecules. In each of these devices, the critical charge transporting interfaces are *buried interfaces* (e.g., organic−insulator, organic−metal, or organic−semiconductor heterojunctions), which are not readily accessible to conventional structural or spectroscopic probes. Though there have been tremendous advancements in molecule-based electronics in the last few years, the difficulty in determining structure−property relationships at buried interfaces has produced a knowledge gap that is a key obstacle to future development. Gaining rigorous and verifiable knowledge of the molecular states involved during the buildup and movement of charge would help to close that gap. More specifically, the relationship between polarons and molecular ions is in need of exploration.

In an attempt to address these questions, we fabricate OTFTs on top of an IR waveguide and apply attenuated total internal reflection Fourier transform infrared (ATR-FTIR) spectroscopy to measure the vibrational spectra (and thus the structure and conformation) of molecules at the buried interfaces, particularly the critically important organic semiconductor−gate dielectric interface. We have demonstrated this approach before for recording vibrational spectra of metal−molecule−metal or metal−molecule−semiconductor tunnel junctions, but without the application of bias voltage.[1] Here, we record FTIR spectra under gate bias voltage to identify spectroscopic signatures unique to gate-induced charge in organic semiconductor thin films.

Infrared spectroscopy has been used in the study of chemical doping[2,3] and electrochemical doping[4,5] of conducting or semiconducting polymers in the bulk form. Two recent studies have applied FTIR to active OTFT devices to gain insight into the conduction mechanisms of OFETs under the application of a gate voltage; these studies revealed chemical species responsible for charge trapping at the dielectric−semiconductor interface[6] and polaron formation within organic semiconductor layers.[7] Optical absorption in other wavelength regions has also been used to probe operating OTFTs, particularly polaron bands from charge injection under gate bias.[8,9] Note that, in principle, there is a Stark effect in the vibrational peak position when an

(1) Jun, Y.; Zhu, X.-Y. *J. Am. Chem. Soc.* **2004**, *126*, 13224−13225.
(2) Chaing, C. K.; Fincher, C. R., Jr.; Park, Y. W.; Heeger, A. J.; Shirakawa, H.; Louis, E. J.; Gau, S. C.; MacDiarmid, A. G. *Phys. Rev. Lett.* **1977**, *39*, 1098−1101.
(3) Kim, J.-Y.; Kim, E.-R.; Sohn, D.; Sakamoto, A.; Tasumi, M. *Bull. Korean Chem. Soc.* **2001**, *22*, 833−836.
(4) Viehbeck, A.; Goldberg, M. J.; Kovac, C. A. *J. Electrochem. Soc.* **1990**, *137*, 1460−1466.
(5) Costantini, N.; Lupton, J. M. *Phys. Chem. Chem. Phys.* **2003**, *5*, 749−757.
(6) Chua, L.-L.; Zaumseil, J.; Chang, J.-F.; Ou, E. C.-W.; Ho, P. K.-H.; Sirringhaus, H.; Friend, R. H. *Nature* **2005**, *434*, 194−199.
(7) Li, Z. Q.; Wang, G. M.; Sai, N.; Moses, D.; Martin, M. C.; Di Ventra, M.; Heeger, A. J.; Basov, D. N. *Nano Lett.* **2006**, *6*, 224−228.
(8) Ziemelis, K. E.; Hussian, A. T.; Bradley, D. D. C.; Friend, R. H.; Ruhe, J.; Wegner, G. *Phys. Rev. Lett.* **1991**, *66*, 2231−2234.
(9) Deng, Y. Y.; Sirringhaus, H. *Phys. Rev. B* **2005**, *72*, 045207.

10.1021/ja070615x CCC: $37.00

intense electric field is applied to a molecular sample;[10] it is too small, however, to be of significance to the kind of experiments presented in this report.

The present study focuses on the identification and quantification of charge-carrying species in OTFTs based on multiple reflection ATR-FTIR. We chose multiple reflection ATR-FTIR[1,6] because it is more sensitive than transmission-based techniques. Charge carrying and trapping species are minorities in an organic semiconductor film. In a typical OTFT device, gate-injected charge carrier density is usually on the order of 10^{13}/cm^2, which is more than 10^2 times lower than the number density of organic semiconductor molecules in an OTFT. To increase charge carrier density for better characterization by ATR-FTIR, we use a polymer electrolyte gate dielectric, lithium perchlorate in poly(ethylene oxide) (PEO). This approach was successfully demonstrated recently to achieve charge carrier densities as high as 10^{15}/cm^2 in OTFTs.[11−13] Such a high charge carrier density results from the high capacitance (on the order of 10 μF/cm^2) due to the presence of mobile ions in the polymer electrolyte dielectric. For comparison, the capacitance of a typical polymer or inorganic dielectric layer is on the order of 10 nF/cm^2. We choose *N*-*N*′-dioctyl-3,4,9,10-perylene tetracarboxylic diimide (PTCDI-C8) as a model system because (1) it is a known *n*-type conductor, (2) it possesses distinctive IR signatures (C═O stretches) that are very sensitive to the charge state of the molecule, and (3) it has been successfully demonstrated in polymer electrolyte gated OTFTs with charge carrier density as high as 6.4×10^{14}/cm^2.[14]

When a charge carrier is injected into an organic semiconductor, there is a strong tendency for it to localize.[15] There are two competing trends for an excited electron in a molecular solid: delocalization and localization. The driving force for delocalization is the resonant electronic interaction characterized by the electron transfer integral between neighboring molecules, β, which determines the electronic bandwidth $\Delta\epsilon_B$ ($\Delta\epsilon_B \approx 4\beta$ in the tight-binding approximation). β is of the order of 10^{1-2} meV in typical molecular solids.[15] The Uncertainty Principle dictates that localization of the electron from a delocalized state is associated with an energetic penalty of δE_{del}, which is approximately equal to half of the electronic bandwidth ($\sim 2\beta$). This is because construction of a localized wavefunction requires the superposition of all delocalized *k* states, corresponding to an average energy approximately in the middle of the conduction band. The driving force for localization comes from polarization in electronic and nuclear coordinates. Electronic polarization occurs on the time scale of the inverse of the Bohr frequency (i.e., $\tau_e \approx 10^{-16}$ to 10^{-15} s), which is shorter than the time scale for the electron to hop from one molecular site to the other (electron hopping time, $\tau_h \approx \hbar/J_M \approx 10^{-14}$ s) and results in an energetic gain of the order of ~1 eV in typical molecular solids. Polarization of nuclear subsystems occurs on longer time scales depending on whether it is intramolecular or lattice motions. Polarization of intramolecular coordinates results in a *small polaron or molecular polaron*; a typical interaction energy of a molecular polaron is 0.1 to 0.2 eV. The molecular polaron usually forms because the molecular vibration time scale ($\tau_v \approx 2 \times 10^{-15}$ to 10^{-14} s) is on the order of or shorter than τ_h. In contrast, a *lattice polaron* does not form because the time scales of optical and acoustic phonons are typically longer than 10^{-13} s and is not competitive with τ_h. The electronic and intramolecular polarization effects lead to an energy gain for localizaion, δE_{pol}, which is dominated by the electronic part. Because of the narrow bandwidth of most molecular solids, the $|\delta E_{del}| < |\delta E_{pol}|$ inequality is usually satisfied. As a result, the formation of a molecular polaron is the norm rather than exception in organic semiconductors.

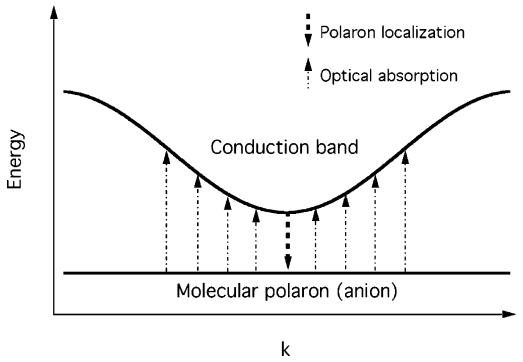

Figure 1. Schematic illustration of a conduction band resulting from delocalized LUMO in an organic semiconductor and a molecular polaron state. The thick dashed arrow represents self-trapping, and the thin dot−dashed arrows illustrate optical absorption in the polaron band.

What do we expect to observe in an IR absorption spectrum for an OTFT under gate bias? To answer this question, let us consider the band structure diagram in Figure 1. When an electron is injected into the conduction band, the strong tendency to localize (thick dashed arrow) leads to a small or molecular polaron, whose energy is independent of the momentum vector (**k**). This is essentially an anion with the excess electron in the lowest unoccupied molecule orbital (LUMO) of the molecule. Even if localization occurs initially in band gap defect states, we also expect polarization to yield a molecular polaron. Thus, we expect two features in IR absorption. The first is vibrational signature unique to an anion; the intramolecular vibrations of an anion are different from those of the neutral molecule because of the changed molecular geometry and force constants. The second is the broad optical absorption (thin dot−dashed arrows) from the lower-lying polaron state to the delocalized conduction band. This polaron band can extend from the IR to the visible region, depending on the extent of polaron stabilization.

Experimental Section

OTFTs were fabricated on Si or Ge semiconductor crystals that served as waveguides for multiple internal reflection ATR-FTIR. Each Si or Ge ATR crystal (10 mm × 50 mm × 1 mm) was cut from a Si (100-mm OD, 1-mm-thick, two side polished, 8−12 Ω•cm^{-1}, EL-CAT Inc.) or Ge (100-mm OD, 1-mm-thick, two side polished, undoped, MTI Corp.) wafer. Each semiconductor crystal was polished to the shape of a parallelogram with 45° angles forming the two ends of the parallelogram. The Si ATR crystal is transparent for $\bar{\nu} \geq 1500$ cm^{-1} while the Ge crystal is transparent down to 500 cm^{-1}.

Thin film transistors were fabricated on the ATR crystals. The surface of each ATR crystal was passivated to provide a hydrophobic wetting layer for organic semiconductor growth. On native oxide terminated silicon, the passivation layer was an octadecyltrichlorosilane self-assembled monolayer, while on germanium the monolayer was formed

(10) Andrews, S. S.; Boxer, S. G. *J. Phys. Chem. A* **2000**, *104*, 11853−11863.
(11) Panzer, M. J.; Newman, C. R.; Frisbie, C. D. *Appl. Phys. Lett.* **2005**, *86*, 103503.
(12) Panzer, M. J.; Frisbie, C. D. *Adv. Funct. Mater.* **2006**, *16*, 1051−1056.
(13) Dhoot, A. S.; Yuen, J. D.; Heeney, M.; McCulloch, I.; Moses, D.; Heeger, A. J. *Proc. Natl. Acad. Sci. U.S.A.* **2006**, *103*, 11834−11837.
(14) Panzer, M. J.; Frisbie, C. D. *J. Am. Chem. Soc.* **2005**, *127*, 6960−6961.
(15) Silinsh, E. A.; Capek, V. *Organic molecular crystals: Interaction, localization, and transport phenomena*; AIP Press: Woodbury, NY, 1994.

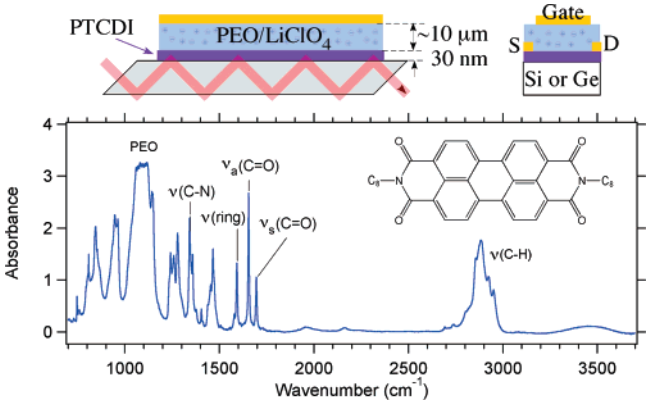

Figure 2. FTIR spectrum for the electrolyte gated device with $V_G = 0$ V. The inset is the molecular structure of PTCDI-C8. (Top) Schematic illustration of the device fabricated on Si or Ge ATR crystals. The device consists of a top gate contact and a PEO/$LiClO_4$ dielectric. S = source; D = drain.

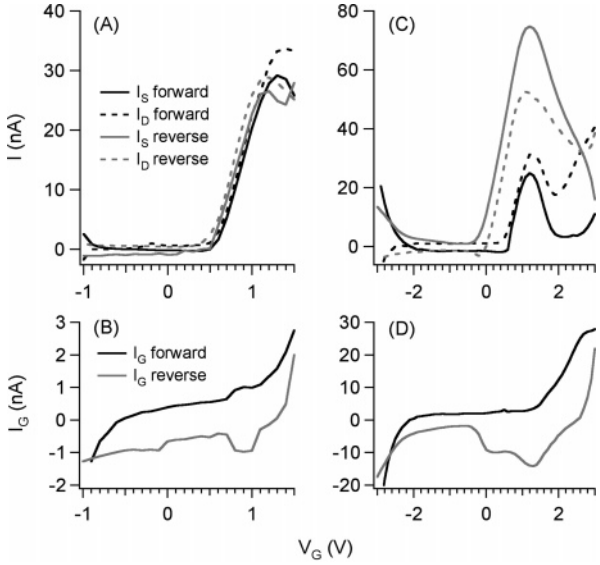

Figure 3. Transistor measurement for a PTCDI-C8 OTFT gated with a polymer electrolyte dielectric. The upper panels show source (I_S, solid) and drain (I_D, dashed) currents, and the lower panels show gate current (I_G) as a function of gate bias, V_G. Panels A and B are from the same low voltage sweep (−1 to 1.5 V). Panels C and D are from the same high voltage sweep (−3 to 3 V). The black and gray curves represent forward and reverse sweeps, respectively.

from a dodecyne hydrogermylation reaction.[16] PTCDI-C8 was vapor-deposited on the passivated Si or Ge surfaces at a rate of 0.05 Å/s to a thickness of 50 Å. Deposition continued at a rate of 0.15 Å/s for an additional 250 Å, giving a total thickness of 300 Å. The substrate temperature during deposition was 110 °C. Gold source and drain electrodes (300 Å thick) were deposited through a shadow mask onto the PTCDI-C8 film at a rate of 0.5 Å/s. The gate dielectric used was an electrolyte solution of $LiClO_4$ in PEO (mw = 10^5) in a ratio of 16 ether oxygen atoms to one lithium ion. The constituents of the dielectric were dissolved in acetonitrile and passed through a 0.2-μm PTFE filter. The solution was then drop cast onto the transistor assembly. Acetonitrile and PTCDI-C8 repel each other because of the high surface energy at their interface, requiring drop casting to occur in a poly(dimethylsiloxane) die. The drop casting procedure produced a PEO film with thickness ~100 μm. After the dielectric was allowed to dry under high vacuum overnight, a 300 Å thick gold gate electrode was deposited onto the dielectric at a rate of 0.5 Å/s. In an attempt to minimize leakage current between the gate and the source or drain electrode, each was aligned to avoid spatial overlap in the horizontal direction.

As a comparison to devices with polymer electrolyte gate dielectric, we fabricated a bottom gate transistor with a conventional polymer gate dielectric layer, polystyrene. In this device, the Si-ATR crystal served both as a waveguide for FTIR spectroscopy and as a gate electrode (with an Al/Au ohmic contact). A 400-nm-thick polystyrene film served as the gate dielectric and was prepared by spin casting it on to a native oxide terminated Si-ATR crystal. A 30-nm-thick PTCDI-C8 film was vacuum-deposited onto the polystyrene surface as described above. This was followed by the deposition of Au source and drain electrodes through a shadow mask.

The top insets in Figure 2 show the device with a polymer electrolyte gate dielectric. The total PTCDI-C8 film area was 4.0 cm^2, whereas the gate area was 2.4 cm^2. The devices fabricated on ATR crystals had source−drain channel dimensions of ~7 mm × 40 mm. For measurement under bias, the sample was connected to a power source and placed in a dry N_2-purged FTIR spectrometer (MIDAC) that was modified for multiple internal reflection with a liquid N_2-cooled MCT detector. During FTIR measurement, a constant voltage (V_G) was applied to the gate electrode, and both the source and the drain electrodes were grounded. The gate voltage was cycled between a maximum and minimum voltage in fixed increments. At each step, the voltage was held at a particular value for 6 min. Each FTIR scan took 5 min and was initiated 1 min after the voltage was applied. All FTIR spectra were collected at an instrument resolution of 1 cm^{-1}. The evanescent wave from the IR light decays exponentially outside the ATR crystal with decay length on the order of the light wavelength. It therefore probes both the PTCDI-C8 layer and the dielectric layer. As an example, Figure 2 shows an FTIR spectrum of the device with polymer electrolyte dielectric at a gate bias of $V_G = 0$ V. The spectrum mainly consists of vibrational peaks due to PTCDI-C8 and PEO molecules. Some of the most distinctive peaks assigned to PTCDI-C8 and PEO are labeled on the spectrum. Details will be discussed later.

Transport properties of the OTFT were measured for similarly fabricated devices on an oxide-terminated silicon substrate, but at smaller lateral dimensions (channel length = 500 μm; width = 50 μm). Details on the transistor measurement were published by Panzer and Frisbie.[14] Briefly, we recorded source (I_S), drain (I_D), and gate (I_G) currents independently as the gate voltage (V_G) was swept and the source−drain bias was set at $V_{SD} = 0.5$ V. In one experiment, V_G was swept between −1 to 1.5 V, and the other from −3 to 3 V. The rate of voltage sweep was 8.5×10^{-2} V/s, which was 2 orders of magnitude faster than that used in FTIR measurements.

Results and Discussion

Details on the electrical performance of PTCDI-C8 transistors with the polymer electrolyte gate dielectrics were published previously.[14] Figure 3 shows measurements for two V_G sweeps. In the low voltage sweep (−1 → 1.5 → −1 V) (Figure 3A), there is little hysteresis in forward and reverse V_G sweeps. The source current (I_S) closely tracks the drain current (I_D), indicating that leakage current is at a very low level, as verified in Figure 3B. The very high effective gate capacitance afforded by the polymer electrolyte dielectric results in a transistor turn-on voltage as low as $V_G = +0.5$ V. The positive turn on voltage corresponds to *n*-channel conduction (i.e., gate-induced electron injection into the PTCDI-C8 layer). For the high voltage sweep (−3 → 3 → −3 V) (Figure 3C), the transistor shows very different behavior. In the forward sweep, the source or drain current peaks at $V_G \approx 1.3$ V and decreases significantly at higher V_G. I_D and I_S start to diverge from each other past this peak, particularly for $V_G > 2$ V, indicating the presence of a significant

(16) Choi, K.; Buriak, J. M. *Langmuir* **2000**, *16*, 7737−7741.

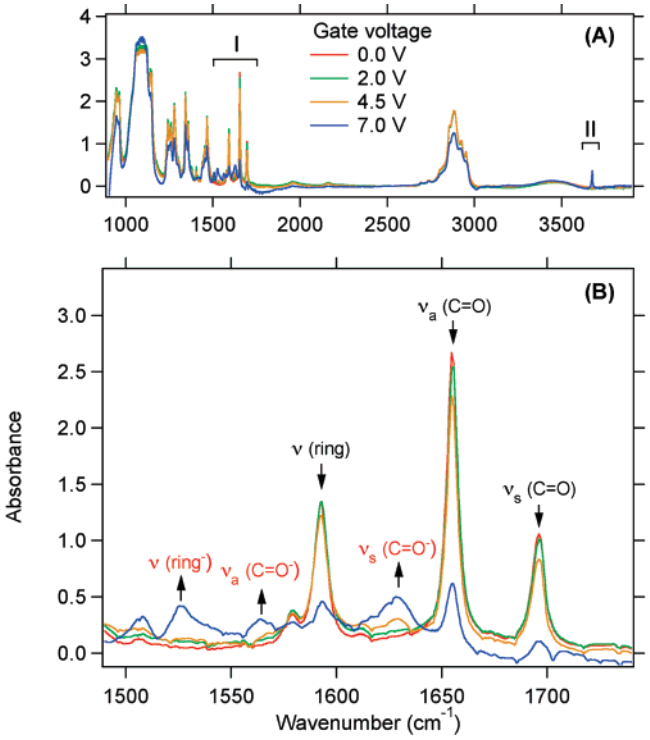

Figure 4. FTIR spectra of the polymer electrolyte gated PTCDI-C8 TFT under various gate bias voltage (red, green, orange, and blue for $V_G = 0.0$, 2.0, 4.5, and 7.0 V, respectively). Peaks labeled with downward arrows decrease with increasing V_G, whereas those with upward arrows increase with V_G. (B) Magnified view of region I in the upper panel.

leakage current, as verified by the rapid rise in I_G (Figure 3D). The reverse sweep shows large hysteresis, and the device becomes irreproducible in subsequent sweeps. For $V_G > 3$ V, there is little source−drain current and leakage current (I_G) dominates (data not shown). Irreversible changes occurred to the OTFT, and subsequent sweeps are very irreproducible. As we show in the following from FTIR measurements, the low gate bias region ($V_G < 2$ V) corresponds to electrostatic doping of the PTCDI layer, whereas the high voltage region ($V_G > 2$ V) corresponds to electrochemical doping (i.e., the diffusion of counterions into the organic lattice).

Figure 4 shows FTIR spectra obtained under various gate biases ($V_G = 0$, 2.0, 4.5, 7.0 V) for a PTCDI-C8 OTFT with a polymer electrolyte dielectric. There are two regions of the spectra that are most sensitive to V_G: (I) 1500−1800 cm^{-1}, corresponding to the C═O stretching and perylene ring stretching modes and (II) a sharp peak at 3677 cm^{-1}, which appears at high gate bias. We initially focus on region I, which is expanded in the lower panel.

Table 1 summarizes major vibrational peaks of neutral PTCDI-C8 (at $V_G = 0$ V), along with those of PEO. The assignments for neutral PTCDI-C8 are from ref 17. For PEO, only peak frequencies are shown and assignments can be found in refs 18 and 19. As shown in Figure 4B, the intensities of the C═O stretching and perylene ring stretching modes associated with the neutral PTCDI-C8 molecule decrease with increasing V_G. This is accompanied by the appearance and growth of a set of new peaks (labeled with red upward arrows) with increasing gate voltage. Following previous solution-phase spectroelectrochemical experiments performed on other diimide molecules,[4] we assign these peaks to the singly charged anion of [PTCDI-C8]$^-$. The two C═O stretching peaks shift downward by 67 and 91 cm^{-1}, respectively, when the neutral PTCDI-C8 molecule is charged with one electron. For comparison, in solution-phase experiments, these peaks shift downward by 78 and 116 cm^{-1} in a smaller model compound, pyromellitic dianhydride-*N*-butylmine (PMDA-*N*-Bu), when it is reduced to the singly charged anion [PMDA-*N*-Bu]$^{-1}$.[4] Further reduction of PMDA-*N*-Bu to [PMDA-*N*-Bu]$^{2-}$ results in a triplet of C═O stretching peaks, with frequency decreases of more than 160 cm^{-1}.[4] On the basis of this previous study of model diimide compounds, we find no evidence of doubly charged [PTCDI-C8]$^{2-}$ in the V_G range investigated. All the new peaks that appeared under positive gate bias and are assigned to [PTCDI-C8]$^-$ are listed in Table 1. As expected from the conversion of neutral PTCDI-C8 to anionic PTCDI-C8 from electron injection under positive gate bias, the decrease in peak intensity associated with neutral PTCDI-C8 peaks is correlated with the increase of the anionic peaks. From repeated sweeping of V_G, we find that there are two regions of V_G in terms of reversibility of the vibrational spectrum: a nearly reversible region for $V_G \leq 2$ V and an irreversible region for $V_G > 2$ V.

Note that the above results focus on the identification and quantification of chemical species formed under gate bias in a polymer electrolyte gated transistor. The main experimental evidence is molecular vibrations (e.g., the C═O stretching modes of neutral and anionic PTCDI-C8 molecules). As shown by Horowitz and co-workers[20,21] and more recently by Li et al.,[7] the formation of molecular polarons gives rise to a weak but broad absorption in the IR region, corresponding to a localized polaron to delocalized band transition. The dot−dashed arrows in Figure 1 illustrate the transitions from the localized polaron state to the delocalized conduction band. We find evidence for this polaron transition in small but detectable changes in the broad background under the more prominent molecular vibrational absorption peaks. Figure 5 shows difference spectra for the polymer electrolyte gated device under various gate biases between 0 and 2 V. In each differential absorbance spectrum at a particular V_G, the absorbance spectrum under zero bias has been subtracted. These differential absorbance spectra reveal the weak and broad polaron band whose intensity increases with gate bias, as expected from the increased density of injected charge. We attribute this broad background feature to the polaron transition, in agreement with Li et al.[7] We do not attempt a quantitative analysis of this polaron band here because of the low signal level as compared to the more prominent changes in vibrational peaks. This is a subject of future study.

In the reversible region, we sweep the gate voltage between 2 and −2 V. Figure 6A plots the absorbance (Abs) of the ν_s(C═O) peak for neutral PTCDI-C8 as a function of V_G for three consecutive cycles of V_G sweeps. Within experimental uncertainty, the absorbance change with V_G is reproducible from sweep to sweep. We make two important observations. The first

(17) Antunes, P. A.; Constantino, C. J. L.; Aroca, R.; Duff, J. *Appl. Spectrosc.* **2001**, *55*, 1341−1346.
(18) Papke, B. L.; Ratner, M. A.; Shriver, D. F. *J. Electrochem. Soc.* **1982**, *129*, 1434−1438.
(19) Yoshihara, T.; Tadokoro, H.; Murahashi, S. *J. Chem. Phys.* **1964**, *41*, 2902−2911.
(20) Horovitz, B. *Solid State Commun.* **1982**, *41*, 729−734.
(21) Horovitz, B.; Osterbacka, R.; Vardeny, Z. V. *Synth. Met.* **2004**, *141*, 179−183.

Table 1. Selected Vibrational Peak Frequencies From FTIR Spectra in Figures 2, 4

PTCDI-C8		PTCDI-C8 anion	
peak/cm^{-1}	vibrational mode	peak/cm^{-1}	vibrational mode
1696	symmetric C═O stretching	1629	symmetric C═O stretching
1655	antisymmetric C═O stretching	1564	antisymmetric C═O stretching
1593	perylene ring stretching	1526	perylene ring stretching
1439	perylene ring stretching	1508	perylene ring stretching
1405	perylene ring stretching	1416	perylene ring stretching
1345	C−N stretching	1325	C−N stretching
1259	C−H perylene bending		
PEO modes (cm^{-1}): 2162, 1960, 1473, 1466, 1453, 1412, 1358, 1343, 1279, 1242, 1145, 1100, 965			

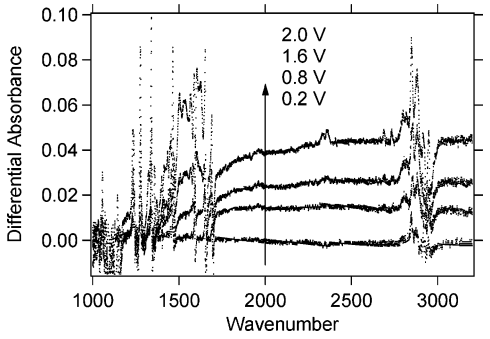

Figure 5. FTIR difference spectra for the polymer electrolyte gated PTCDI-C8 device under various gate biases (V_G = 0.2, 0.8, 1.6, 2.0 V) in the electrostatic doping region. In each differential absorbance spectrum at a particular V_G, the absorbance spectrum at V_G = 0 V has been subtracted.

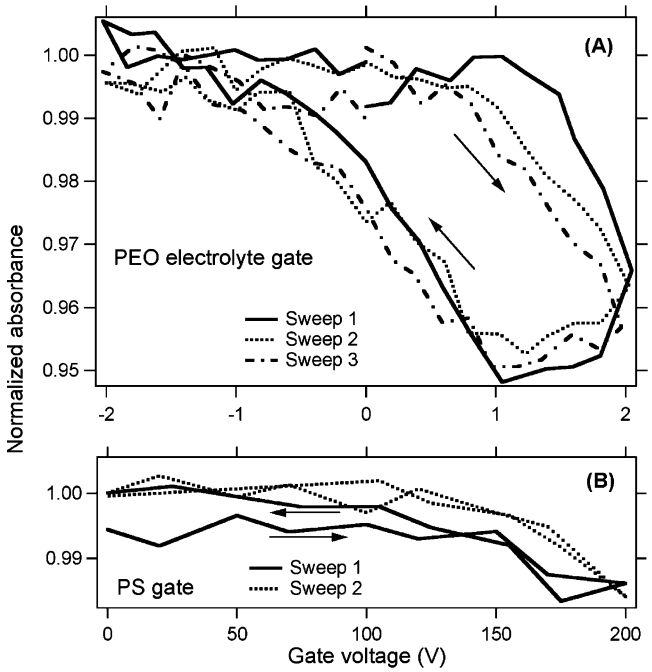

Figure 6. Normalized absorbance of the ν_s(C═O) mode of neutral PTCDI-C8 as a function of gate voltage for the polymer electrolyte gated TFT (A) and the polystyrene gated TFT (B). The arrows indicate the sweep directions. There are three V_G sweeps (0 → 2 → 0 → −2 → 0 V) in (A) and two sweeps (0 → 200 → 0 V) in (B).

observation is the complete recovery of the ν_s(C═O) peak intensity when the gate voltage is decreased from 2 to −2 V, indicating that all PTCDI-C8 anions are converted back to the neutral molecules. The second observation is the presence of significant hysteresis; the Abs vs V_G data points during the reverse sweep (2 → 0 V) are below those of the forward sweep (0 → 2 V). Complete recovery only occurs when V_G is swept into the negative region. These observations are consistent with electrostatic doping of the PTCDI-C8 film gated by the polymer electrolyte dielectric in which time-dependent diffusion occurs over observable timescales. Upon the application of a gate bias voltage, the positive Li^+ ions must diffuse to the PEO/PTCDI-C8 boundary to establish the electric field at the dielectric−organic semiconductor interface. The field-induced diffusion of ions in the polymer electrolyte is a slow process, and the observed hysteresis reflects diffusion kinetics. In addition, the sample geometry used in the present study amplifies hysteresis: the area of the organic semiconductor film under gate bias is 60% of the total area, and polarization of PTCDI-C8 molecules outside the gated area may be a slow process. For comparison, hysteresis in transistor measurements (Figure 3A) was much smaller. We attribute this to the much smaller lateral dimension of the device used in transistor measurements than that used in FTIR spectroscopy. Note that measurements in this reversible region were carried out on a newly fabricated device and V_G never exceeded the (−2 → 2 V) range.

On the basis of the changes in absorbance, we can calculate the density of gate-induced charge in the PTCDI-C8 film, given the proportionality relationship between absorbance and molecular concentration. As shown in Figure 6A, the application of V_G = 2 V results in the conversion of 4.6 ± 0.2% neutral PTCDI-C8 molecules to the anionic form. The total area of PTCDI-C8 film sample is 4 cm^2, whereas the gate size is 2.4 cm^2. Assuming that charge injection induced by electrostatic field only occurs under the gate, 7.7% of the PTCDI-C8 film is reduced. Since the density of PTCDI-C8 molecules in a monolayer is 2.5 × 10^{14} cm^{-2} and the interplane distance of the PTCDI-C8 film is 20 Å,[22,23] the calculated film density is 1.25 × 10^{21} cm^{-3}. Given a total PTCDI-C8 film thickness of 30 nm, we calculate a charge injection density of 2.9 ± 0.2 × 10^{14} cm^{-2}. The charge injection density achieved here is equivalent to the complete conversion of an entire monolayer of PTCDI-C8 molecules at the interface. For comparison, the injected charge density estimated from the integrated gate current in electrical measurement was 6.4 × 10^{14} cm^{-2} at V_G = 2 V.[14] We believe the electrical measurement may overestimate the charge injection density due to the possible presence of both gate leakage current and ion diffusion current.

As a comparison to the polymer electrolyte gated OTFT, we also carried out FTIR measurements for a PTCDI-C8 TFT with a 400-nm-thick polystyrene dielectric. As expected, the amount of change observed in the FTIR spectra under gate bias is significantly smaller than that seen for the polymer electrolyte

(22) Chesterfield, R. J.; McKeen, J. C.; Newman, C. R.; Ewbank, P. C.; Demetrio, A. S. F.; Bredas, J.-L.; Miller, L. L.; Mann, K. R.; Frisbie, C. D. *J. Phys. Chem. B* **2004**, *108*, 19281−19292.
(23) Hadicke, E.; Graser, F. *Acta Crystallogr.* **1986**, *C42*, 189−195.

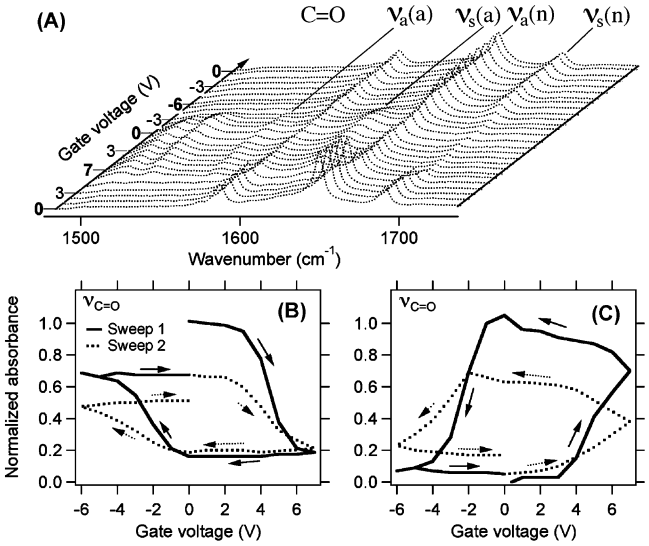

Figure 7. (A) FTIR spectra in carbonyl stretching region for a complete V_G sweep ($0 \rightarrow 7 \rightarrow 0 \rightarrow -6 \rightarrow 0$ V). The symmetric and asymmetric C═O stretching peaks are labeled, and (n) and (a) stand for neutral and anionic PTCDI-C8, respectively. Normalized absorbance of the symmetric C═O stretching peaks of neutral (B) and anionic (C) PTCDI-C8 as a function of V_G for two sweeps. The arrows indicate the direction of voltage sweeps.

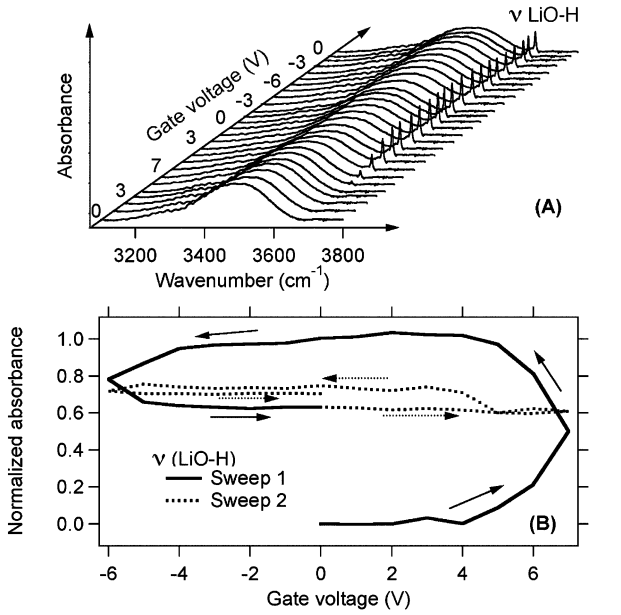

Figure 8. (A) FTIR spectra in the OH stretching region as a function of gate voltage. The broad peak centered at about 3500 cm^{-1} is assigned to hydrogen-bonded water in PEO. The sharp peak at 3677 cm^{-1} is assigned to LiO−H. (B) Normalized (to the maximum) absorbance of the ν(LiO−H) peak as a function of V_G for two voltage sweeps. The arrows indicate the V_G sweep directions.

gated OTFT. Figure 6B plots the absorbance of the ν_s(C═O) peak for neutral PTCDI-C8 as a function of V_G up to 200 V, above which dielectric breakdown is observed. At the maximum gate voltage of $V_G = 200$ V, $1.2 \pm 0.3\%$ of the neutral molecules have been converted to anions, corresponding to a charge injection density of $4.5 \pm 2 \times 10^{13}$ cm^{-2}. This maximum doping level is equivalent to the conversion to anions of 18% of a monolayer of PTCDI-C8 molecules at the interface, more than 5× lower than the charge injection density in the PEO system at $V_G = 2$ V.

When V_G exceeds 2 V in the polymer electrolyte gated device, transistor measurements revealed a large hysteresis in the source and drain currents and a rapid increase in gate current (Figure 3C,D). FTIR reveals irreversible changes to the PTCDI-C8 film. Figure 7A shows a set of FTIR spectra taken as V_G is cycled in the range $0 \rightarrow 7 \rightarrow 0 \rightarrow -6 \rightarrow 0$ V, with ±1 V steps (each data point corresponds to the voltage held for 6 min). The corresponding peak intensities (integrated and normalized to the maximum value) of ν_s(C═O) for the neutral and anionic PTCDI-C8 species are shown in the lower panels. As V_G increases above 3 V, the sharp decrease in the intensity of the neutral PTCDI-C8 peak is accompanied by a sharp increase in the intensity of the anionic peak. The concentration of the neutral PTCDI-C8 molecule decreases to 18% of its starting value at $V_G = 6$ to 7 V. Since 40% of the PTCDI-C8 molecules are not directly under the gate electrode, this result indicates that reduction occurs for not only all PTCDI-C8 molecules under the gate electrode but also some PTCDI-C8 molecule beyond the gated area.

There are two types of irreversibility in the Abs vs V_G plots in Figure 7. The first is the large hysteresis in the neutral and anionic peak intensities within each V_G sweep ($0 \rightarrow 7 \rightarrow 0 \rightarrow -6 \rightarrow 0$ V). After the nearly complete reduction of PTCDI-C8 at $V_G = 6$ to 7 V, the neutral species showed virtually no sign of recovery until the gate voltage is less than 0 V. At negative V_G, partial recovery occurs, as shown by the increase in neutral peaks and the decrease in anionic peaks. The second type of irreversibility is the change from cycle to cycle. As shown by the neutral PTCDI-C8 peak intensity in Figure 7B, 30% of the neutral PTCDI-C8 intensity is lost after V_G is returned to zero after negative bias. Following the second sweep, another 20% of the intensity is lost. Interestingly, the loss in the intensity of neutral PTCDI-C8 molecules from sweep to sweep is not compensated for by a gain in that of anionic species. In fact, there is less anionic PTCDI-C8 intensity formed in the second sweep than in the first sweep.

The irreversible loss of C═O stretching peak intensities for both neutral and anionic PTCDI-C8 molecules following each cycle of V_G sweep must be due to chemical reaction. Supporting this conclusion, we find a sharp peak at 3677 cm^{-1} at high V_G values (see region II in Figure 4A). This peak is the O−H stretching mode in a lithium hydroxide molecule (LiOH).[24] Figure 8 shows in detail the O−H stretching region of FTIR spectra during the first sweep of gate voltage. The broad peak present in all spectra is the O−H stretching mode of hydrogen-bonded water in the PEO electrolyte. When $V_G \geq 5$ V, the sharp LiO−H vibrational peak appears. Repeated cycling of the voltage causes only small changes in LiOH concentration, as shown by the small change in absorbance following the second cycle of V_G sweep, lower panel. This LiOH molecule giving rise to the 3677 cm^{-1} peak must be located in the PTCDI-C8 film; otherwise, it should dissociate in the PEO electrolyte layer. We arrive at two conclusions: (1) Li^+ must diffuse into the PTCDI-C8 thin film at sufficiently positive V_G and (2) there is a chemical degredation reaction that occurs in the PTCDI-C8 layer to form LiOH.

The intercalation of Li^+ into layered solids is well known, particularly for materials used in lithium ion batteries. It is not surprising that, under sufficiently positive gate bias, Li^+ diffuses into the layered solid of PTCDI-C8. To form a LiOH molecule,

(24) Wickersheim, K. A. *J. Chem. Phys.* **1959**, *31*, 863−869.

the presence of H_2O is required, and water is a readily available impurity in the hydrophilic PEO layer. It is then likely that as Li^+ ions diffuse into the PTCDI-C8 layer at $V_G > 2$ V, they carry water molecules along with them in the form of a hydration shell. In view of the loss of C═O stretching peak intensity in both neutral and anionic PTCDI-C8 and the irreversible formation of LiOH, we propose the following reaction mechanism in eq 1. In this reaction, the PTCDI-C8 anion reacts with H_2O impurities to give OH^-, which readily associates with Li^+ to form the LiOH molecule.

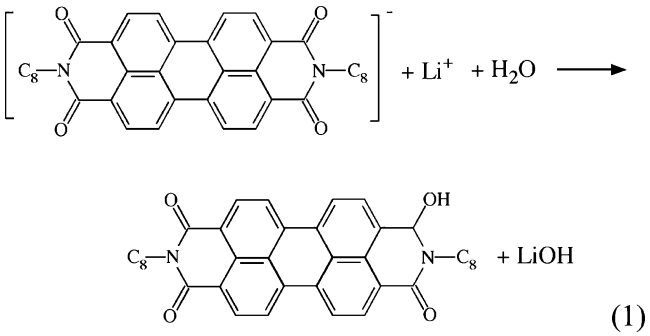

(1)

The mechanism for PTCDI-C8 anion formation in the irreversible region at $V_G > 2$ V is completely different from the electrostatic mechanism at $V_G \leq 2$ V. At $V_G > 2$ V, we essentially have electrochemical reduction of PTCDI-C8 molecules with Li^+ as counterions. Thus, this is called electrochemical doping. The existence of two distinctively different regimes of doping is most obvious in the first part of the voltage sweep ($0 \rightarrow 7$ V) in Figure 7. The rate of conversion from neutral to the anionic species (as a function of V_G) increases dramatically when V_G exceeds 2 V. The negative slope of the Abs vs V_G plot for neutral PTCDI-C8 (Figure 7B) or the positive slope for PTCDI-C8 anion (Figure 7C) is proportional to the capacitance of the dielectric. The capacitance of the dielectric is basically constant for $V_G = 0-2$ V. This is the electrostatic doping region. For $V_G > 2$ V, the effective capacitance (slope) increases in a discontinuous fashion and reaches a value that is more than 1 order of magnitude larger than that in the electrostatic doping region. This is because, in addition to electrostatic doping, the more efficient electrochemical doping mechanism is turned on for $V_G > 2$ V. The transition from the electrostatic to the electrochemical doping region is irreversible because of the partial trapping of Li^+ in the PTCDI-C8 layer and the chemical reaction proposed above.

The spectroscopic evidence for the two doping regions observed here in a polymer electrolyte gated OTFT is consistent with previous electric measurements that established the two doping regions: (1) the electrostatic (also called ion-blocking or non-Faradaic[25]) region[11−14] where the ionic double layer at the electrolyte−organic semiconductor interface is responsible for charge injection into the first few layers of the organic semiconductor at the dielectric interface and (2) the electrochemical (also called ion-permeable or Faradaic[25]) region[26,27] involving the oxidation/reduction of the whole organic semiconductor thin film and the intercalation of counterions into the organic semiconductor layer. A transition between these two regions has also been reported recently by Lin and Lonergan in electrical measurement of a liquid electrolyte gated TFT of polyacetylene as the active organic semiconductor layer.[25]

Conclusions

We successfully applied ATR-FTIR spectroscopy to directly probe active layers in OTFTs. For a PTCDI-C8 TFT with a PEO/$LiClO_4$ polymer electrolyte gate dielectric, FTIR spectroscopy showed the formation of anionic PTCDI-C8 species from electron injection under positive gate bias. There were two distinctively different doping regions: a reversible and electrostatic doping region for $V_G \leq 2$ V, and an irreversible and electrochemical doping regime for $V_G > 2$ V. In the electrostatic doping region, the injected electron density at $V_G = 2$ V was $2.9 \pm 0.2 \times 10^{14}$ cm^{-2}, corresponding to the conversion of slightly more than one monolayer of PTCDI-C8 molecules into anions. Transistor measurements taken in this regime are reversible with little hysteresis. In the electrochemical doping region at $V_G > 2$ V, we observed the diffusion of Li^+ into the organic semiconductor film and the conversion of all PTCDI-C8 molecules into anionic species. In addition, we observed a chemical reaction between anionic PTCDI-C8 and impurity water molecules. Transistor measurements in this regime reveal large hysteresis and discrepancies in source and drain currents, the latter stemming primarily from a large gate leakage current. For comparison, we also probed a PTCDI-C8 TFT with a conventional polystyrene gate dielectric; the maximum charge carrier density under electrostatic doping at $V_G = 200$ V was $4.5 \pm 2 \times 10^{13}$ cm^{-2}, corresponding to the conversion of 18% of one monolayer of PTCDI-C8 molecules into anions.

Acknowledgment. This work was supported by the U.S. Department of Energy under Grant No. DE-FG02-05ER46252 and the National Science Foundation MRSEC Program under Award No. DMR 0212302.

JA070615X

(25) Lin, F.; Lonergan, M. C. *Appl. Phys. Lett.* **2006**, *88*, 133507.
(26) Ofer, D.; Crooks, R. M.; Wrighton, M. S. *J. Am. Chem. Soc.* **1990**, *112*, 7869−7879.
(27) Taniguchi, M.; Kawai, T. *Appl. Phys. Lett.* **2004**, *85*, 3298−3300.